

INJECTION DIAGNOSTIC PROCEDURES FOR THE CHALK RIVER SUPERCONDUCTING CYCLOTRON

W.G. Davies

Atomic Energy of Canada Limited, Chalk River Nuclear Laboratories
Chalk River, Ontario, Canada K0J 1J0

The beam diagnostics system for the injection beam line for the Chalk River Tandem Accelerator - Superconducting Cyclotron is described. The system has been designed such that simple and easily interpreted measurements can be made for operational beam monitoring as well as for the complete 6-dimensional beam phase-space determinations required for beam development.

1. Introduction

The Chalk River Tandem Accelerator-Superconducting Cyclotron project (TASCC) consists of a 13 MV tandem injecting into a $K=520$ ($\text{MeV}\cdot\text{A}/\text{Q}^2$) superconducting cyclotron. In order to minimize the radial and axial betatron amplitudes, and to maximize the quality of the extracted beam, precise 6-dimensional emittance matching to the cyclotron is required. Thus a well designed beam diagnostics system is an important part of achieving an emittance match to the cyclotron. Having the right information can save enormous amounts of time, both during initial commissioning and regular operation. The problem of making and interpreting the beam measurements that are necessary for a) new beam development, b) routine monitoring of the beam during operation, is the topic of this paper.

2. The Diagnostic System

The injection system for the cyclotron is shown in Fig. 1. The figure indicates all the major functions of the injection system and the locations of all diagnostic devices. The devices used are seven rotating wire beam profile monitors (BPM), two pulsed beam monitors (PBM) which measure the bunch length, a precision beam emittance measuring device, (ED) and several slit and Faraday cup systems (SI), as indicated. The outputs of all of these devices can be transmitted to the control computer in digital form.

The principle diagnostic elements are located at five stations that perform distinct functions as follows (see Fig. 1).

- 1) To match the tandem beam to the requirements of the beam analysis system. Horizontal and vertical waists are produced at SI2 and the center of QI3 respectively. The transverse emittance can be measured as required for beam development.
- 2) To match the longitudinal phase space to the requirements at the HEB (high-energy buncher). The LEB (low-energy buncher) amplitude, the effective drift length to the stripper in the tandem terminal and the mean stripper straggling can be measured.
- 3) To produce waists of the correct size at W1 (horizontal) and W2 (vertical). These waists are transformed to the cyclotron center (stripper) by diagonal transfer matrices when the cyclotron matching system is correctly adjusted. Accurate measurements of the areas and orientation of the horizontal and vertical phase-space ellipses are made here.

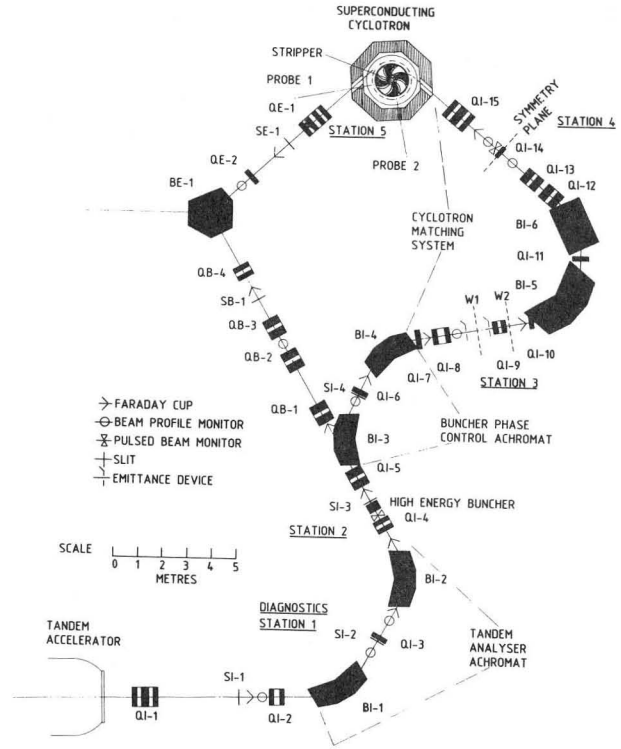


Fig. 1 Layout of the Chalk River Superconducting Cyclotron Laboratory.

- 4) To determine both the transverse and longitudinal beam emittances at the symmetry plane at QI14 for beam development. A "rapid" diagnostics mode can be employed for operational monitoring.
- 5) To determine that the correct transverse emittance match has been achieved and that the injection system is achromatic at the cyclotron stripper.

3. Transverse Measurements at Stations 1 and 4

The arrangement at QI3 and QI14 is shown in Fig. 2. In both cases two BPM's are used that have reflection symmetry about the center of the lens. This symmetry results in greatly simplified equations, improved accuracy, and a simple interpretation of the measurements. Simplicity is very important for operational monitoring.

The mean-square widths (σ_1^2 and σ_3^2) are calculated from the digitized beam profiles measured at positions (1) and (3) (Fig. 2). The beam properties at (2) are related to those at (1) and (3) as follows:

$$\sigma_1 = R^{-1} \sigma_2 T_R^{-1} \tag{1}$$

and

$$\sigma_3 = M \sigma_2^T M \tag{2}$$

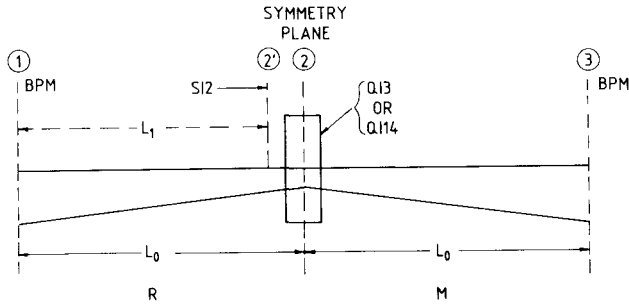


Fig. 2 Schematic representation of the diagnostic system at QI3 and QI14. Both systems employ two BPM's placed symmetrically about the center of the lens. At station 1 there is also the slit SI2.

where the phase ellipse formalism of Brown⁴ is used. If $R = M_{refl}$, then in the standard notation[†]

$$R_x = \begin{bmatrix} M_{22} & M_{12} \\ M_{21} & M_{11} \end{bmatrix} \text{ and } R_x^{-1} = \begin{bmatrix} M_{11} & -M_{12} \\ -M_{21} & M_{22} \end{bmatrix} \quad (3)$$

with similar matrix transformations for the vertical (y) plane.

This leads to two highly symmetric equations in the three unknowns x_2, r_2, θ_2 in both the x and y planes respectively as follows:

$$x_1^2 = M_{11}^2 x_2^2 - 2M_{11}M_{12}r_2x_2\theta_2 + M_{12}^2\theta_2^2 \quad (4a)$$

$$x_3^2 = M_{11}^2 x_2^2 + 2M_{11}M_{12}r_2x_2\theta_2 + M_{12}^2\theta_2^2 \quad (4b)$$

with similar equations relating y_i^2, ϕ_i^2 and r_{yi} to the equivalent matrix elements for the y-plane.

This information is sufficient for operational monitoring because $r_2=0$ in the y-plane and is nearly zero in the x-plane at both QI3 and QI14. Thus $y_1^2=y_3^2$ and $x_1^2 \approx x_3^2$. Since the emittances

$$\epsilon_x = x\theta [\sqrt{1-r_x^2}]^{1/2} \text{ and } \epsilon_y = y\phi [\sqrt{1-r_y^2}]^{1/2} \quad (5)$$

are known rather accurately from the measurements at station 3. Eq. (4) can be solved with the help of eq. (5) yielding

$$x_2^2 = [(x_3^2 + x_1^2) - \sqrt{Z^2}] / [4 M_{11}^2] \quad (6a)$$

$$\theta_2^2 = [(x_3^2 + x_1^2) + \sqrt{Z^2}] / [4 M_{12}^2] \quad (6b)$$

$$r_2 = [F^2 / (1 + F^2)]^{1/2} \quad (6c)$$

where $F = (x_3^2 - x_1^2) / (4 M_{11}M_{12}\epsilon_x)$ (6d)

and $Z^2 = (x_3^2 + x_1^2) - (4 M_{11}M_{12}\epsilon_x)^2 / (1-r_2^2)$ (6e)

[†] Because the optical system is non-dispersive between points (1) and (3) the x and y transforms can be represented by 2 x 2 matrices.

We see that $r_2 \approx F$ when $r_2 \ll 1$ further simplifying the calculations.

The x-waist in region 1 occurs at SI2, and the slit width provides additional information, (i.e. slit width $w = 4x_2'$). Use of this information breaks the symmetry inherent in eq. 4, but can lead to improved accuracy, especially when combined with the procedures to be described in the following paragraphs.

During the development of new beams, it will be necessary to achieve the maximum possible accuracy. Further information can be obtained by measuring the beam width at position (3) (Fig. 2) as a function of the lens strength QI3 or QI14[†]. It will usually be sufficient to make two measurements, one with the lens on and one with it off. Now we have two systems of equations of the type shown in eq. 4, where the transfer matrix elements are different for each lens setting. This new system of equations is best solved by least squares. This makes it easy to add more measurements as necessary, but even more importantly gives a direct estimate of the errors in the desired quantities. Equations (4) are transformed to the form

$$x_j^2 = f_j(x_2, \theta_2, r_2), \quad j=1,2,3 \quad (7)$$

where we solve for x_2, θ_2, r_2 directly. This form leads to more stable solutions and eliminates the possibility of imaginary solutions. From these extended measurements, both the x and y plane phase ellipses (x, θ, r_x) and (y, ϕ, r_y) can be obtained as well as the phase space areas ϵ_x and ϵ_y .

In region 1, this information is used in a straightforward manner to adjust the three elements of QI1 to produce x and y-plane waists at SI2 and at the center of QI3 with the correct aspect ratios.

During routine operation, the measurements in region 4, will be used to monitor that the beam properties remain correct. During commissioning and new beam development, complete emittance measurements will be made and used as described in section 7.

4. Longitudinal Emittance at Stations 2 and 4

Measurement of the longitudinal phase space at Station 2 is used to i) adjust the LEB amplitude to produce a time waist at the tandem stripper, ii) measure the stripper straggling and optimize stripper thickness, iii) measure the longitudinal beam emittance at the HEB. The latter information is used to set the nominal HEB amplitude.

The geometrical relationships for this system⁵ are indicated in Fig. 3. The bunch length at PBMI³ is measured as a function of the LEB amplitude K_0 and the stripper-gas pressure P. Because the optical system is achromatic² between the LEB and PBMI, the system can be represented by 2 x 2 matrix transforms.

The beam matrix at the tandem stripper is

$$\sigma_1 = M_1 \sigma_0^T M_1 \quad (8a)$$

[†] The focusing power of the lenses have been calibrated to 0.1% over their operating range.

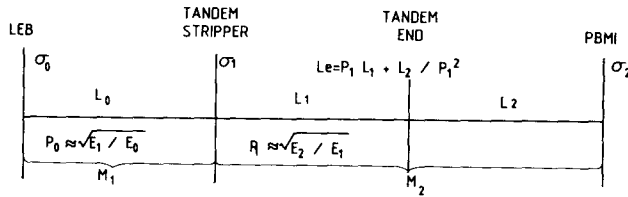


Fig. 3 Schematic representation of the diagnostics system for adjusting the low-energy buncher. The important variables are indicated.

where

$$M_1 = \begin{bmatrix} P_0 & 0 \\ 0 & 1/P_0^2 \end{bmatrix} \begin{bmatrix} 1 & L_0 \\ 0 & 1 \end{bmatrix} \begin{bmatrix} 1 & 0 \\ K_0 & 1 \end{bmatrix} \quad (8b)$$

The beam matrix at PBM1 can be written as

$$\sigma_2 = M_2 \sigma_1^T M_2^T \quad (9a)$$

where (see eq. 8b)

$$M_2 = L_2 P_1 L_1 \quad (9b)$$

$$\sigma_1^T = \sigma_1 + \delta_s^2 \quad (9c)$$

where δ_s^2 is related to the stripper straggling³.

On expanding eq. 9a, we obtain the following equation, relating the unknown parameters to the measurement of the mean square bunch length λ_2^2 .

$$\lambda_2^2 = \left\{ \left[P_1 P_0 (1 + K_0 L_0) \right]^2 + \frac{2 P_1}{P_0} L_e K_0 (1 + K_0 L_0) + \frac{L_e^2}{P_0^4} K_0^2 \right\} \lambda_0^2 + \left\{ (P_1 P_0 L_0)^2 + 2 \frac{P_1}{P_0} L_e L_0 + \frac{L_e^2}{P_0^4} \right\} \delta_0^2 + L_e^2 \delta_s^2 \quad \text{where } \delta_s^2 = K_1 P + K_2 P^2 \quad (10)$$

For light ions, where $\delta_s^2 \ll (k_0 \lambda_0)^2$, a minimum of 3, but preferably 5 measurements of λ_2^2 as a function of K_0 will provide adequate accuracy for the measured parameters λ_0 , δ_0 and L_0 . In fact, L_0 can be calculated independently from a model of of the tandem and $\lambda_0 \approx \beta \lambda / 4 \sqrt{3}$. However, because L_0 is rather sensitive to the details of the voltage gradient in the tandem the present method is more accurate.

For heavy ions, 11 measurements will usually be made to determine λ_0 , δ_0 , L_0 , K_1 and K_2 . This seems complicated and time consuming. However, the LEB, the stripper gas pressure and the PBM, are all computer controlled and the data accumulation takes only a few seconds per point.

Once the parameters have been determined, the longitudinal phase-space ellipse at the HEB is found with the help of eq. 8 and 9. Correct adjustment of the LEB amplitude, the stripper-gas pressure and the HEB amplitude follow directly from these measurements.

The longitudinal emittance is measured at station 4 using an analogous procedure to the above. The bunch length, λ_1 , is measured at PBM2 as a function of the HEB amplitude, and the phase space at the HEB and station 4 are related by an equation identical to 8a, where now M_1 must be a 4 x 4 matrix⁴ because the system is dispersive. Thus we obtain a system of equations of the form

$$\lambda_1^2 = M_{31}^2 x_0^2 + M_{32}^2 \theta_0^2 + M_{33}^2 \lambda_0^2 + 2 M_{33} M_{34} (r_0 \lambda_0 \delta_0) + M_{34}^2 \delta_0^2 \quad (11)$$

where $M_{33} = (1 + K_0 L_e)$ and $M_{34} = L_e$; K_0 is now the HEB strength and L_e the effective length from SI3 to PBM2. The x_0 and θ_0 terms are constant, thus L_e can be accurately determined from a least squares fit of eq. 11 to say three measurements since λ_0 , δ_0 and r_0 are known from the measurements at PBM1. The longitudinal phase ellipse at QI14 is obtained from the equivalent of eq. 8a with the parameters obtained from fitting eq. 11.

5. Beam Emittance Measurements in Region 3

A conventional "double-slit-type"⁶ emittance device is used here to obtain accurate transverse beam emittance information. Details of the apparatus and data reduction methods are described in ref. 6. The 68%, 95% and RMS emittance contours will be obtained. The true RMS contour is needed so the results are compatible with those calculated in section 3.

During normal operation, these measurements will be used to guide the adjustment of lenses Q17 and Q18 to produce an X-waist at W1 and a Y-waist at W2 with the correct aspect ratios. During commissioning and the development of new beams, information gained here will be used as described in section 7.

6. Diagnostics in the Cyclotron, Station 5

The diagnostic tools in the cyclotron are the two radial probes¹, which are separated by 90° (Fig. 1). With the stripper foil out and the RF off, it turns out that the radial "phase shift" between probes 1 and 2 is still nearly 90° for all beams. (It depends upon the ratio of the injection radius of curvature to the radius of the inner equilibrium orbit which in turn depends on the ratio of charge-states before and after stripping.) Thus the equation connecting probes 1 and 2 is to a good approximation

$$x_2^2 = M_{12}^2 \theta_1^2 + M_{14}^2 \delta_1^2 \quad (12a)$$

where $M_{12} \approx 0.5 \text{ mm/mrad}$, $M_{14} \approx 5 \text{ mm/\%}$. Thus since

$\delta_1 \leq 0.05\%$ we obtain immediately that

$$\theta_1 = \left[(x_2^2 - M_{14}^2 \delta_1^2) / M_{12}^2 \right]^{1/2} \approx x_2 / M_{12} \quad (12b)$$

The r-coefficient can be found from eq. 5 and the value of ϵ_x obtained in section 5 i.e.

$$r = + \left[1 - (\epsilon_x / x_1 \theta_1)^2 \right]^{1/2} \quad (12c)$$

The resolution of the probes in the radial direction is 0.2 mm.

In the axial (y) direction the situation is more complicated. The equation connecting the probes has the form

$$y_2^2 = y_1^2 + 2L(ry\phi)_1 + L^2\phi_1^2 \quad (13)$$

where $L \approx 0.8$ m. The resolution of the probes in the axial direction is only 3 mm. Thus to obtain reasonable information about the axial phase space of the beam at the stripper, we must make several measurements of y_1 and y_2 as a function of QI8 and QI14 and fit these results with the constraint that ϵ_y is constant, where ϵ_y is taken from the measurements of section 5.

Once the x and y-plane phase-space ellipses have been determined, the phase space at the stripper is obtained from the relation

$$\sigma_s = M_{1s}^{-1} \sigma_1^T M_{1s}^{-1} \quad (14)$$

where M_{1s} is a matrix with a phase shift of about 17° in the radial plane and is a drift with a length $L \approx 15$ cm in the axial plane.

7. Diagnostics Procedures for Cyclotron Matching

The measurements at stations 4 and 5 required to assure correct emittance matching to the cyclotron acceptance are interrelated and can be made concurrently. A match has been achieved when the transfer matrix is achromatic between W1 and the cyclotron stripper (Fig. 1) and when it is a diagonal unit matrix in the transverse elements. The procedure is as follows:

- i) The phase space is measured at stations 3, 4, 5 as described earlier for 3 settings of QI8, nominal and $\pm 50\%$ of nominal. In the process we obtain 6 measurements at station 5 since QI14 is switched on and off to obtain complete information at station 4.
- ii) With nominal settings, the beam momentum is varied $\Delta P \approx \pm 0.2\%$ and the beam centroid shifts at stations 4 and 5 are measured.
- iii) The longitudinal phase space is measured at station 4.

This information can be used to check that the transfer matrix is correct between W1 and QI14 (M_{34}), QI14 and the cyclotron stripper (M_{45}), and W1 to the stripper (M_{35}) as follows. The emittance values at each station are related by the equation

$$\sigma_j = M_{ji} \sigma_i^T M_{ji} \quad (15)$$

where j,i refer to station numbers. There are 9 unknowns in the x-plane and 4 in the y-plane, but these unknowns are not all independent. They are constrained by the condition that $\det |M| = 1$ in both x and y and the relation

$$\begin{bmatrix} \ell_x = M_{31} \\ \ell_\theta = M_{32} \end{bmatrix} = \begin{bmatrix} M_{21} & -M_{11} \\ M_{22} & -M_{12} \end{bmatrix} \begin{bmatrix} d_x = M_{14} \\ d_\theta = M_{24} \end{bmatrix} \quad (16)$$

which connects the dispersion with the path length matrix elements in the x-plane. Thus we have 6 independent parameters in x and 3 in y. In the y-plane, we obtain the following system of equations

$$y_j^2 = M_{11}^2 y_i^2 + 2M_{11}M_{12}(r_i y_i \phi_i) + R_{12}^2 \phi_i^2 \quad (17a)$$

$$\phi_j^2 = M_{21}^2 y_i^2 + 2M_{21}M_{22}(r_i y_i \phi_i) + R_{22}^2 \phi_i^2 \quad (17b)$$

$$M_{11}M_{22} - M_{21}M_{11} = 1 \quad (17c)$$

The unknown matrix elements are found from a least squares fit of the matrix element to the data from procedure 7i) subject to eq. 17c.

In the x-plane, the equations are more complicated because the dispersive matrix elements must also be found, but the method is the same.

At station 4, the dispersive matrix elements are found directly from procedure 7ii)

$$\begin{aligned} d_x &= \Delta x / \Delta p \\ d_\theta &= \Delta \theta / \Delta p \end{aligned}$$

where Δx and $\Delta \theta$ are the centroid shifts, not RMS widths.

The matrix element $M_{34} = L_e$ (see eq. 11) is also determined directly from procedure 7ii).

At the center of the cyclotron, the analysis is more complicated, because the dispersive and path length matrix elements are more difficult to determine accurately. However, when the system is correctly adjusted $\Delta x_1 = 0$ and $\Delta x_2 = M_{14} \Delta p$ (see section 6). This is a "null" condition and provides a very sensitive test of achromaticity.

Space does not permit a more complete description of how this information will be used to achieve a match, but it is evident that knowledge of M_{34} , M_{45} and $M_{35} = M_{34}M_{45}$ provides an excellent way of identifying any "faulty" area and gives important clues to the nature of the faults.

A statistical "prediction analysis" has been made for the procedures described here and shows that the measurements do indeed provide meaningful information and a powerful basis for efficient beam development and good operational monitoring.

References

- 1) J.H. Ormrod et al., 7th Int. Conf. on Cycl., Zürich; J.S. Fraser and P.R. Tunnicliffe, AECL-4913 (1973) and J. Ormrod et al., these Proceedings.
- 2) W.G. Davies and A.R. Rutledge, IEEE Trans. on Nucl. Sci., NS-26, No.2, April 1979, p.2086.
- 3) W.G. Davies, Proc. 9th Int. Conf. on Cycl. and Applications, CAEN, France, Sept. 1981, p.349; Pub. by Editions de Physique, Les Ulis, France.
- 4) K.L. Brown, SLAC Report #75, 1967 and #91, 1970 and W.G. Davies, AECL-8053, 1983.
- 5) J.M. Brennan, private communication.
- 6) Ch. Egelhaaf et al., IEEE, NS-24, No.3, p.1745 and R.L. Graham, informal report, TASC-1-08-02, AECL 1983.

Acknowledgements

The author would like to thank J.H. Ormrod and E.A. Heighway for helpful discussions, and T.K. Alexander, J.S. Geiger, F.J. Sharp, J.J. Hill, A.S.C. Hyde and P.J. Jones for procuring, installing and commissioning the diagnostics hardware.